

Published in final edited form as:

AJNR Am J Neuroradiol. 2017 December ; 38(12): 2385–2390. doi:10.3174/ajnr.A5360.

Anterior mesencephalic cap dysplasia: novel brainstem malformative features associated with Joubert syndrome

Filippo Arrigoni, MD¹, Romina Romaniello, MD², Denis Peruzzo, PhD¹, Alberto De Luca, PhD^{1,3}, Cecilia Parazzini, MD⁴, Enza Maria Valente, MD, PhD^{5,6}, Renato Borgatti, MD², and Fabio Triulzi, MD⁷

¹Neuroimaging Lab, Scientific Institute IRCCS Eugenio Medea, Bosisio Parini, Italy

²Neuropsychiatry and Neurorehabilitation Unit, Scientific Institute IRCCS Eugenio Medea, Bosisio Parini, Italy

³Department of Information Engineering, University of Padova, Padova, Italy

⁴Department of Pediatric Radiology and Neuroradiology, Children Hospital “V. Buzzi”, Milan, Italy

⁵Department of Molecular Medicine, University of Pavia, Pavia, Italy

⁶Neurogenetics Unit, IRCCS Santa Lucia Foundation, Rome, Italy

⁷Department of Neuroradiology, Scientific Institute IRCCS Cà Granda Foundation—Ospedale Maggiore Policlinico, Milan, Italy

Abstract

In Joubert syndrome, the “molar tooth” sign can be associated to several additional supra and infratentorial malformations. Here we report on three subjects (two siblings, age: 8-14 years) with Joubert syndrome, showing an abnormal thick bulging of the anterior profile of the mesencephalon causing a complete obliteration of the interpeduncular fossa. DTI revealed that the abnormal tissue consists of an ectopic white matter tract with a latero-lateral transverse orientation. Tractographic reconstructions support the hypothesis of impaired axonal guidance mechanisms as responsible for the malformation. The two siblings were compound heterozygous for two missense variants in the TMEM67 gene, while no mutations in a panel of 120 ciliary genes were detected in the third patient. The name “anterior mesencephalic cap dysplasia”, referring to the peculiar aspect of the mesencephalon on sagittal MRI, is proposed for this new malformative feature.

Introduction

The “molar tooth” sign is the distinctive imaging feature and a mandatory criterion for the diagnosis of Joubert syndrome (JS), a rare group of conditions characterized by a complex malformation of the midbrain-hindbrain. Molar tooth sign owes its name to the appearance of the pons and superior cerebellar peduncles (SCP) on axial MR images, resembling a

Corresponding author: Filippo Arrigoni, MD, Postal address: Neuroimaging Lab, Scientific Institute IRCCS Eugenio Medea, Via Don Luigi Monza 20, 23842 Bosisio Parini, Italy, filippo.arrigoni@bp.inf.it, Phone: +39031877398.

Submission to meetings: These data have been accepted as oral communication at the ESNR Meeting 2017 that will be held in Malmö (Sweden) in September

molar tooth. It is related to a moderate to severe vermian hypo-dysplasia, associated with a narrow pontine-mesencephalic junction and thickened, elongated, horizontal SCP1.

The typical clinical signs of JS (episodic hyperpnea, abnormal eye movements, developmental delay and ataxia²) may be associated with heterogeneous neurologic and non-neurologic symptoms and defects in other organs, including the kidneys, retina, liver and skeleton^{1,3,4}, giving rise to an extremely large spectrum of phenotypes, from relatively mild to severe conditions⁵.

JS is part of an expanding group of disorders called ciliopathies, that are caused by dysfunction of the primary cilium, an ubiquitous subcellular organelle that plays a key role in brain development and in many cellular functions⁶. To date, more than 35 genes, encoding for proteins of the primary cilium or its apparatus, have been identified as causing JS^{5,7}, however many patients remain undiagnosed, suggesting further genetic heterogeneity.

The variable degree of vermian hypo-dysplasia and the presence of associate supratentorial findings (hippocampal malrotation, callosal dysgenesis, migration disorders, hypothalamic hamartomas, cephaloceles, and ventriculomegaly) may further complicate the spectrum^{8,9}.

We here report on three patients from two different families (two male brothers with genetically defined JS, and one unrelated female), presenting an additional complex malformation of the brainstem characterized by an abnormal thick bulging of the anterior profile of the mesencephalon. DTI revealed that the abnormal tissue consists of an ectopic bundle of white matter with a latero-lateral transverse orientation, likely resulting from impaired axonal guidance mechanisms during the early stages of brain development.

Materials and Methods

Neuroimaging data

Patients underwent MR imaging studies on either 3 T (patients 1 e 2) or 1.5 T (patient 3) scanners at two different Institutions (E. Medea Research Institute and V. Buzzi Children Hospital). Axial and coronal T2-weighted images (thickness: 3 mm), axial and coronal FLAIR (thickness: 3 mm) and 3D T1-weighted SPGR (voxel size: 1 mm³) were acquired. Balanced-SSFP sequence were acquired at 3T to evaluate cranial nerves. High-resolution DTI data (voxel size: 2mm³; b-values: 0, 300, 1100 s/mm²; number of directions: 32) were available for the 2 patients examined at 3T, while the third patient had low-resolution DTI (voxel size: 3mm³; b-values: 0, 1100 s/mm²; number of directions: 15).

DTI data were pre-processed with the DIFFPREP module of TORTOISE to remove motion and eddy current artifacts, then correction of geometrical EPI distortions was performed with DR-BUDDI using the dual phase encoding acquisition¹⁰. Fiber tractography was performed with Trackvis¹¹ in patient 1 and 2. We did not perform tractography in patient 3 because of the lower quality (i.e. signal-to-noise ratio, resolution) of the data.

Clinical and genetic data

Neurological, neuropsychological and instrumental evaluations as well as genetic analysis were carried out in all patients.

The local Ethics Committee approved the study. Written informed consent was obtained from all participating families.

Results

Neuroimaging

The three patients showed a complex brainstem and cerebellar malformation, with normal findings in the supratentorial brain.

The main features of the common midbrain-hindbrain malformation were the following:

- a severe vermian hypo-dysplasia with thickened, horizontal SCP determining a molar-tooth shape of the superior brainstem on axial images (Fig1);
- a flattening of inferior olives and medullary pyramids (Fig1);
- a narrow isthmus, with thin pontine-mesencephalic junction;
- a thickened tectum on sagittal plane in patient 1;
- an abnormal bulging of the anterior profile of the mesencephalon on sagittal planes. On axial images, such bulging resulted in a complete obliteration of the interpeduncular fossa, giving to the mesencephalon a more rounded anterior profile. Interestingly, the ectopic mass had the same signal intensity of white matter in all MR weightings and it did not look as a single, nodular interpeduncular structure (Fig1);
- the III, V, VI, VII and VIII cranial nerves could be recognized. Trochlear nerves were not identified probably because of technical limits; extraocular muscles, including oblique superior muscles, appeared regular in terms of signal intensity and volume. Optic nerves were thinned in patient 3;
- cranial nerves IX and X could be detected on Balanced-SSFP sequence in patient 1 and 2. Patient 1 showed an agenesis of the left XII nerve. Lower cranial nerves could not be assessed in patient 3;
- color-encoded DTI maps and tractography reconstructions revealed that the anterior mesencephalic bulging corresponded to a transverse orientated white matter tract in the interpeduncular cistern (Fig2). On tractography, an apparent merging of corticospinal (CSTs) with the abnormal mesencephalic bundle could be suspected;
- on color-encoded DTI maps, CSTs could be regularly recognized only till the upper part of the pons (Fig2). On tractography, pontine transverse fibers and middle cerebellar peduncles appeared as a thick unique bundle anteriorly displaced in the pons (Fig3). SCP were thickened, while inferior cerebellar

peduncles were atrophic in one case. SCPs decussation was absent in patients 1 and 2 and it was thinned in patient 3.

Genetic findings

Clinical and genetic findings of the two siblings were reported in 2009, as part of a molecular genetic screening of the *TMEM67* gene in patients with JS. They both resulted to be compound heterozygous for *TMEM67* missense variants c. 1115C>A/p.(T372K) and c. 2345A>G/p.(H782R), which were inherited from the healthy father and mother, respectively (Family COR32 in Brancati et al.12). The third patient underwent next-generation-sequencing based analysis of a panel of 120 ciliopathy-related genes 13, which failed to identify any pathogenic variant.

Clinical findings

Patient 1 is now a 14-year-old male. He had impaired psychomotor development, with delayed motor acquisitions (able to walk independently at 6 years of age) and absence of expressive language. Nowadays he can use signs language and is able to read and write words in capital letters. Good social skills are present. Neurological examination showed diffuse hypotonia, nystagmus, ocular-motor apraxia, dysmetria, severe oral-motor dyspraxia and gait ataxia. Cognitive testing showed moderate intellectual disability (WISC III-R IQ=46 at performance sub-items). Visual assessment detected a reduced visual acuity and bilateral optical nerve coloboma. Unilateral polycystic kidney (right) with progressive atrophy and compensatory hypertrophy of the contralateral was evident on kidney ultrasound. Liver biopsy at the age of 8 years documented congenital hepatic fibrosis associated with mild portal hypertension, normal liver functioning and absence of esophageal varices.

Patient 2 is an 8-year-old male. As the older brother, he had delayed psychomotor development, walking unaided at the age of 3 years and lacking any expressive language. Nowadays he uses sign language with good social interactions and skills. Diffuse hypotonia, dysmetria, oral-motor dyspraxia and gait ataxia with moderate intellectual disability (Performance IQ=41) are evident at neurological examination. A liver biopsy performed at 4 years of age demonstrated congenital hepatic fibrosis, hepatosplenomegaly, portal hypertension and small esophageal varices. He also had an increase of transaminase and γ GT levels and thrombocytopenia secondary to hypersplenism.

Patient 3 is a 11-years old female, the only child of consanguineous healthy parents (second grade cousins). She presented early in life with mild motor delay, severe intellectual impairment, marked visual deficit and nystagmus. On the latest neurological examination, she presented severe intellectual disability with poor expressive language and social skills, diffuse hypotonia and clumsiness. She had severe visual impairment (1/50 bilaterally), nystagmus and roving ocular movements. Fundus oculi showed nerve optic hypoplasia and small vessels, and electroretinogram could not elicit any response. Abdominal ultrasound and audiometric evaluations were normal.

Clinical findings and instrumental evaluation are summarized in Supplementary Table 1.

Discussion

The presence of an anterior mesencephalic bulging due to an ectopic transverse white matter bundle represents a new malformative pattern of the midbrain for which we propose the name “anterior mesencephalic cap dysplasia” (AMCD). Such definition is adopted and adapted from a previously described malformation of the brainstem, pontine tegmental cap dysplasia¹⁴, which shares some common features with AMCD. In both cases the sagittal profile of the brainstem shows an abnormal “cap” that in AMCD is located anteriorly, at mesencephalic level, while in pontine tegmental cap dysplasia is located posteriorly at pontine level. Moreover, in both cases, on axial sections and DTI, the cap looks like a white matter ectopic bundle with a transverse latero-lateral orientation.

Other diagnosis, like tumors, metastasis or other proliferative disorders could be easily excluded considering their signal intensity and expansive/infiltrative features.

The presence of an interpeduncular mass in patients with JS was previously reported by Harting et al.¹⁵, who described 3 patients with a nodular structure within the interpeduncular fossa. Similar tissue can also be depicted, but not commented on, in a couple of papers by Huppke et al.¹⁶ and Alorainy et al.¹⁷. Probably interpeduncular masses in JS represent a continuum, but we believe that, according to their appearance on both morphological sequences and DTI, a distinction between pedunculated and non-pedunculated structures can be maintained. IH is a nodular structure, isointense to gray matter, with a rounded shape and a peduncle that connects the mass to the brainstem, while AMCD is isointense to white matter, has no peduncle and completely fills the interpeduncular fossa. Moreover, in AMCD DTI confirmed the presence of an ectopic transverse white matter bundle anterior to the mesencephalon. Interestingly, according to tractographic reconstructions, the bundle appears to be in continuity with corticospinal tracts (CST) and may represent an ectopic decussation of motor tracts. Careful interpretation of these findings is needed because the algorithm we used for tractography has limitations in resolving crossing or sharply angulated fibers¹⁸, which are better handled by more sophisticated approaches, as HARDI. Unfortunately, because of the characteristics of our protocol (low b-values, few diffusion directions), spherical deconvolution based tractography did not improve the resolution of the tracts.

Anomalies in tract decussations (both CST and SCP) have been frequently described in neuropathological reports of JS patients^{19–23}. Moreover, the absence of CST decussation has been described in other conditions like occipital encephalocele, Dandy-walker malformation, Möbius syndrome, horizontal gaze palsy and progressive scoliosis, L1 Syndrome, Kallmann Syndrome and trisomy 18,^{24,25} while there is no report of aberrant ectopic mesencephalic decussation.

More recently, Poretti et al.⁹ described a convex protuberance of the ventral contour of the midbrain due to a nodular structure in 13/110 JS, expanding the findings from Hartling¹⁵. No DTI data are showed and the lesions are interpreted as grey matter heterotopias, however the possibility of ectopic white matter projections is left open.

Only a single case was previously reported of a JS fetus of 22 weeks of gestation, showing AMCD both at MRI and post-mortem histology²⁶. As in our patients, in utero and histology-based tractography confirmed the abnormal projection of CST into the interpeduncular cistern. It is to note that both in the fetal case and in our patients motor tracts were atrophic/barely recognizable in the pons and medulla. The alternative hypothesis that the abnormal mesencephalic bundle represents an ectopic, aberrant white matter tract connecting either the cerebral or cerebellar hemispheres cannot be completely discarded, even if it is not supported by tractography. We also hypothesized that the tract could represent the decussation of SCP displaced anteriorly, but in patient 3 SCP decussation was present (even if uncommon in JS, the persistence of SCP decussation is not exceptional as it was already reported in neuropathological studies²¹) and in the two siblings we could not identify a direct connection between SCP and the bundle. Pathology confirmation is needed to fully understand the course of the abnormal tract and its origin.

Mirror movements, that are often associated with abnormal pyramidal decussation resulting in bilateral CST projections to the spinal cord were not detected in our patients²⁷. Functional MRI during motor tasks would be of help to verify the decussation of CST, but could not be performed due to the insufficient cooperation of patients.

The two siblings carried mutations in the *TMEM67* gene, a ciliary gene which is expressed in brain midline, hindbrain, retina, kidney, liver, and developing sphenoid bone and plays a fundamental role in centriole migration to the apical membrane and formation of the primary cilium²⁸. Interestingly *TMEM67* represents the gene for which the strongest gene-phenotype correlates have been drawn^{29–31}. In fact, nearly all *TMEM67*-mutated JS patients present with congenital liver fibrosis, variably associated to optic nerve or chorioretinal coloboma, retinal dystrophy and renal involvement (COACH syndrome)^{32–34}.

Mounting evidences suggest a central role for the primary cilia in modulating neurogenesis, cell polarity, axonal guidance and possibly adult neuronal functions^{5,6}. The lack of decussation of CST and SCP reported in neuropathological as well as DTI tractography studies of patients with JS suggested that defective primary cilia could also impair the process of axonal guidance, and the presence of an aberrant/ectopic white matter tract in patients with a proven ciliopathy can further support this theory.

Aberrant or ectopic white matter tracts have been detected in a wide spectrum of brain malformations involving brainstem and corpus callosum^{26,35–40} as a result of defects in axonal guidance or other mechanisms. The advent of high-resolution MRI and DTI along with the advances in genetic technologies helped to define and expand human disorders of axon guidance and will probably contribute to the discovery of many additional similar conditions in the future.

Conclusions

Through high-resolution MRI, DTI and tractography, we demonstrated that non-pedunculated interpeduncular tissue in JS may represent an ectopic transverse white matter tract located in the mesencephalon, for which the name “AMCD” is proposed.

Supplementary Material

Refer to Web version on PubMed Central for supplementary material.

Acknowledgments

We are grateful to patients and their family for the cooperation to this study.

Funding:

This work was funded by the Italian Ministry of Health (Ricerca Corrente 2016-17) and by ERC STarting Grant 260888

Abbreviations list

JS	Joubert syndrome
SCP	superior cerebellar peduncles
CST	cortico-spinal tracts

References

1. Romani M, Micalizzi A, Valente EM. Joubert syndrome: congenital cerebellar ataxia with the molar tooth. *Lancet Neurol.* 2013; 12:894–905. [PubMed: 23870701]
2. Joubert M, Eisenring JJ, Robb JP, et al. Familial agenesis of the cerebellar vermis. A syndrome of episodic hyperpnea, abnormal eye movements, ataxia, and retardation. *Neurology.* 1969; 19:813–25. [PubMed: 5816874]
3. Zaki MS, Abdel-Aleem A, Abdel-Salam G, et al. The molar tooth sign: a new Joubert syndrome and related cerebellar disorders classification system tested in Egyptian families. *Neurology.* 2008; 70:556–65. [PubMed: 18268248]
4. Valente EM, Brancati F, Dallapiccola B. Genotypes and phenotypes of Joubert syndrome and related disorders. *Eur J Med Genet.* 2008; 51:1–23. [PubMed: 18164675]
5. Mitchison HM, Valente EM. Motile and non-motile cilia in human pathology : from function to phenotypes. *J Pathol.* 2017; 241:294–309. [PubMed: 27859258]
6. Engle EC. Human Genetic Disorders of Axon Guidance. *Cold Spring Harb Perspect Biol.* 2010; 2:a001784. [PubMed: 20300212]
7. Vilboux T, Doherty DA, Glass IA, et al. Molecular genetic findings and clinical correlations in 100 patients with Joubert syndrome and related disorders prospectively evaluated at a single center. *Genet Med.* 2017 Jan 26. [Epub ahead of print].
8. Poretti A, Huisman TAGM, Scheer I, et al. Joubert syndrome and related disorders: spectrum of neuroimaging findings in 75 patients. *AJNR Am J Neuroradiol.* 2011; 32:1459–63. [PubMed: 21680654]
9. Poretti A, Snow J, Summers AC, et al. Joubert syndrome: neuroimaging findings in 110 patients in correlation with cognitive function and genetic cause. *J Med Genet.* 2017 Jan 13. [Epub ahead of print].
10. Pierpaoli, C., Walker, L., Irfanoglu, MO., Barnett, A., Basser, P., Chang, LC., Koay, C., Pajevic, S., Rohde, G., Sarlls, J., W, M. Tortoise: an integrated software package for processing of diffusion MRI data. *Proceedings of International Society of Magnetic Resonance in Medicine*; 2010. p. 1597
11. R, W., Benner, T., AG, S., et al. Diffusion Toolkit: A Software Package for Diffusion Imaging Data Processing and Tractography. *Proceedings of International Society of Magnetic Resonance in Medicine*; 2007. p. 3720

12. Brancati F, Iannicelli M, Travaglini L, et al. MKS3/TMEM67 mutations are a major cause of COACH Syndrome, a Joubert Syndrome related disorder with liver involvement. *Hum Mutat.* 2009; 30:E432–42. [PubMed: 19058225]
13. Roosing S, Romani M, Isrie M, et al. Mutations in CEP120 cause Joubert syndrome as well as complex ciliopathy phenotypes. *J Med Genet.* 2016; 53:608–15. [PubMed: 27208211]
14. Barth PG, Majoie CB, Caan MWA, et al. Pontine tegmental cap dysplasia : a novel brain malformation with a defect in axonal guidance. *Brain.* 2007; 130:2258–66. [PubMed: 17690130]
15. Harting I, Kotzaeridou U, Poretti A, et al. Interpeduncular heterotopia in Joubert syndrome: a previously undescribed MR finding. *AJNR Am J Neuroradiol.* 2011; 32:1286–9. [PubMed: 21636654]
16. Huppke P, Wegener E, Bohrer-Rabel H, et al. Tectonic gene mutations in patients with Joubert syndrome. *Eur J Hum Genet.* 2015; 23:616–20. [PubMed: 25118024]
17. Alorainy IA, Sabir S, Seidahmed MZ, et al. Brain Stem and Cerebellar Findings in Joubert Syndrome. *J Comput Assist Tomogr.* 2006; 30:116–21. [PubMed: 16365585]
18. Jeurissen B, Leemans A, Tournier J-D, et al. Investigating the prevalence of complex fiber configurations in white matter tissue with diffusion magnetic resonance imaging. *Hum Brain Mapp.* 2013; 34:2747–66. [PubMed: 22611035]
19. Friede RL, Boltshauser E. Uncommon syndromes of cerebellar vermis aplasia. I: Joubert syndrome. *Dev Med Child Neurol.* 1978; 20:758–63. [PubMed: 729929]
20. Yachnis AT, Rorke LB. Neuropathology of Joubert syndrome. *J Child Neurol.* 1999; 14:655–72. [PubMed: 10511338]
21. Ferland RJ, Eyaid W, Collura RV, et al. Abnormal cerebellar development and axonal decussation due to mutations in AH11 in Joubert syndrome. *Nat Genet.* 2004; 36:1008–13. [PubMed: 15322546]
22. Juric-Sekhar G, Adkins GJJ, Doherty D, et al. Joubert syndrome : brain and spinal cord malformations in genotyped cases and implications for neurodevelopmental functions of primary cilia. *Acta Neuropathol.* 2012; 123:695–709. [PubMed: 22331178]
23. Poretti A, Boltshauser E, Loenneker T, et al. Diffusion tensor imaging in Joubert syndrome. *AJNR Am J Neuroradiol.* 2007; 28:1929–33. [PubMed: 17898198]
24. Miyata H, Miyata M, Ohama E. Pyramidal tract abnormalities in the human fetus and infant with trisomy 18 syndrome. *Neuropathology.* 2014; 34:219–26. [PubMed: 24313853]
25. Ten Donkelaar HJ, Lammens M, Wesseling P, et al. Development and malformations of the human pyramidal tract. *J Neurol.* 2004; 251:1429–42. [PubMed: 15645341]
26. Mitter C, Jakab A, Brugger PC, et al. Validation of In utero Tractography of Human Fetal Commissural and Internal Capsule Fibers with Histological Structure Tensor Analysis. *Neuroanat.* 2015; 9:164.
27. Welniarz Q, Dusart I, Roze E. The corticospinal tract: Evolution, development, and human disorders. *Dev Neurobiol.*
28. Dawe HR, Smith UM, Cullinane AR, et al. The Meckel-Gruber Syndrome proteins MKS1 and meckelin interact and are required for primary cilium formation. *Hum Mol Genet.* 2007; 16:173–86. [PubMed: 17185389]
29. Smith UM, Conugar M, Tee LJ, et al. The transmembrane protein meckelin (MKS3) is mutated in Meckel-Gruber syndrome and the wpk rat. *Nat Genet.* 2006; 38:191–6. [PubMed: 16415887]
30. Baala L, Khaddour R, Saunier S, et al. The Meckel-Gruber Syndrome Gene, MKS3, Is Mutated in Joubert Syndrome. *Am J Hum Genet.* 2007; 80:186–94. [PubMed: 17160906]
31. Suzuki T, Miyake N, Tsurusaki Y, et al. Molecular genetic analysis of 30 families with Joubert syndrome. *Clin Genet.* 2016; 90:526–35. [PubMed: 27434533]
32. Otto EA, Tory K, Attanasio M, et al. Hypomorphic mutations in meckelin (MKS3/TMEM67) cause nephronophthisis with liver fibrosis (NPHP11). *J Med Genet.* 2009; 46:663–70. [PubMed: 19508969]
33. Iannicelli M, Brancati F, Mougou-Zerelli S, et al. Novel TMEM67 mutations and genotype-phenotype correlates in meckelin-related ciliopathies. *Hum Mutat.* 2010; 31:E1319–31. [PubMed: 20232449]

34. Bachmann-Gagescu R, Phelps IG, Dempsey JC, et al. KIAA0586 is Mutated in Joubert Syndrome. *Hum Mutat.* 2015; 36:831–5. [PubMed: 26096313]
35. Poretti A, Meoded A, Rossi A, et al. Diffusion tensor imaging and fiber tractography in brain malformations. *Pediatr Radiol.* 2013; 43:28–54. [PubMed: 23288476]
36. Briguglio M, Pinelli L, Giordano L, et al. Pontine Tegmental Cap Dysplasia: developmental and cognitive outcome in three adolescent patients. *Orphanet J Rare Dis.* 2011; 6:36. [PubMed: 21651769]
37. Haller S, Wetzel SG, Lutschg J. Functional MRI, DTI and neurophysiology in horizontalgaze palsy with progressive scoliosis. *Neuroradiology.* 2008; 50:453–9. [PubMed: 18214457]
38. Caan MWA, Barth PG, Niermeijer J-M, et al. Ectopic peripontine arcuate fibres, a novel finding in pontine tegmental cap dysplasia. *Eur J Paediatr Neurol.* 2014; 18:434–8. [PubMed: 24485946]
39. Sicotte NL, Salamon G, Shattuck DW, et al. Diffusion tensor MRI shows abnormal brainstem crossing fibers associated with ROBO3 mutations. *Neurology.* 2006; 67:519–21. [PubMed: 16894121]
40. Arrigoni F, Romaniello R, Peruzzo D, et al. Aberrant supracallosal longitudinal bundle: MR features, pathogenesis and associated clinical phenotype. *Eur Radiol.* 2015; 26:2587–96. [PubMed: 26560723]

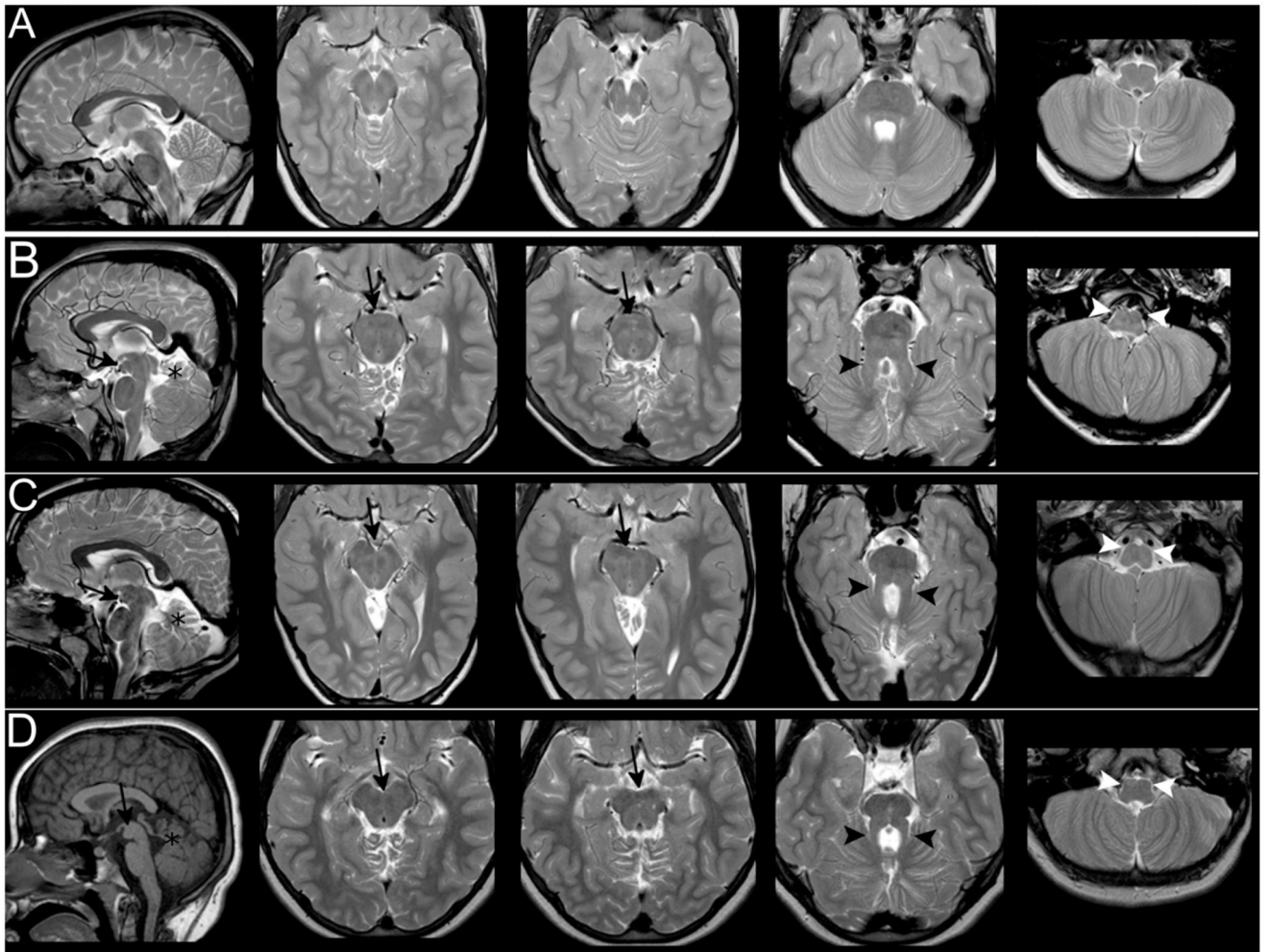


Figure 1. Morphological findings.

Images show T1 and T2-weighted sagittal and axial sections of a normal subject (Row A), patient 1 (Row B), patient 2 (Row C) and patient 3 (Row D). In the three patients, the mesencephalon shows an anterior bulging (black arrows) that fills the interpeduncular cistern visible both on sagittal and axial sections. The signal intensity of the abnormal mass is similar to white matter. Patients also share the classical features of MTS: cerebellar hypodysplasia (black stars), thickened and horizontal SCP (black arrowheads) and hypoplasia of medullary pyramids and inferior olivary nuclei (white arrowheads).

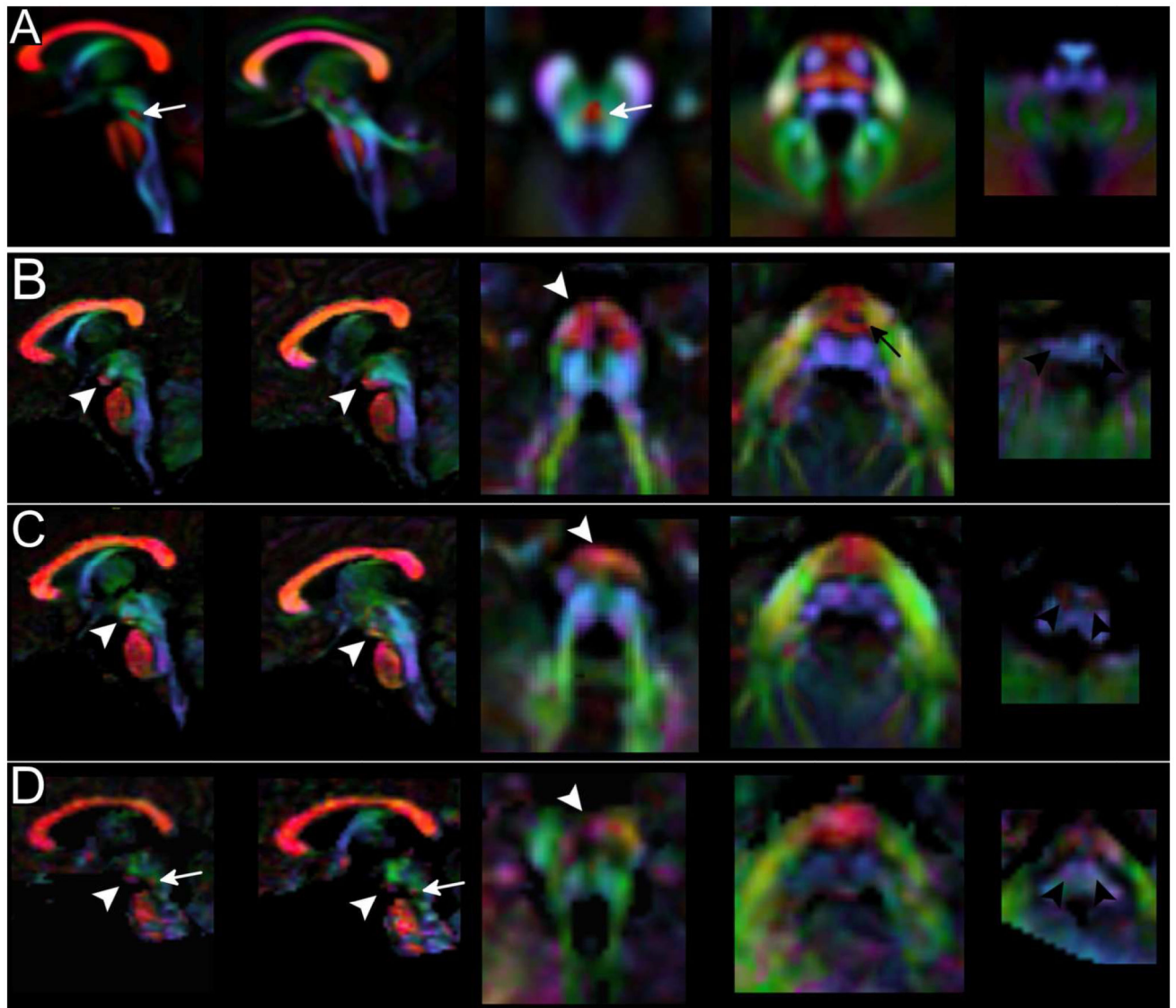


Figure 2. Color-coded DTI maps

On color-coded maps patients 1 (Row B), 2 (Row C) and 3 (Row D) show an altered organization of white matter tracts if compared to a template of normal subjects (Row A). The anterior bulging of the mesencephalon corresponds to an area of transverse-oriented diffusivity located anteriorly in the interpeduncular fossa (white arrowheads). CST in the pons are thinned (black arrow) or non-clearly recognizable and transverse pontine fibers appear as a unique bundle displaced in the anterior part of the pons. In the medulla, CST and lemnisci are hypoplastic/atrophic and olives reduced in volume. The decussation of SCP (white arrow in the normal template) is absent in patient 1 and 2 and markedly thinned in patient 3 (white arrow in D). [Color legend: red, green and blue represent areas of respectively transverse, antero-posterior and caudo-cranial orientation of diffusivity and white matter]

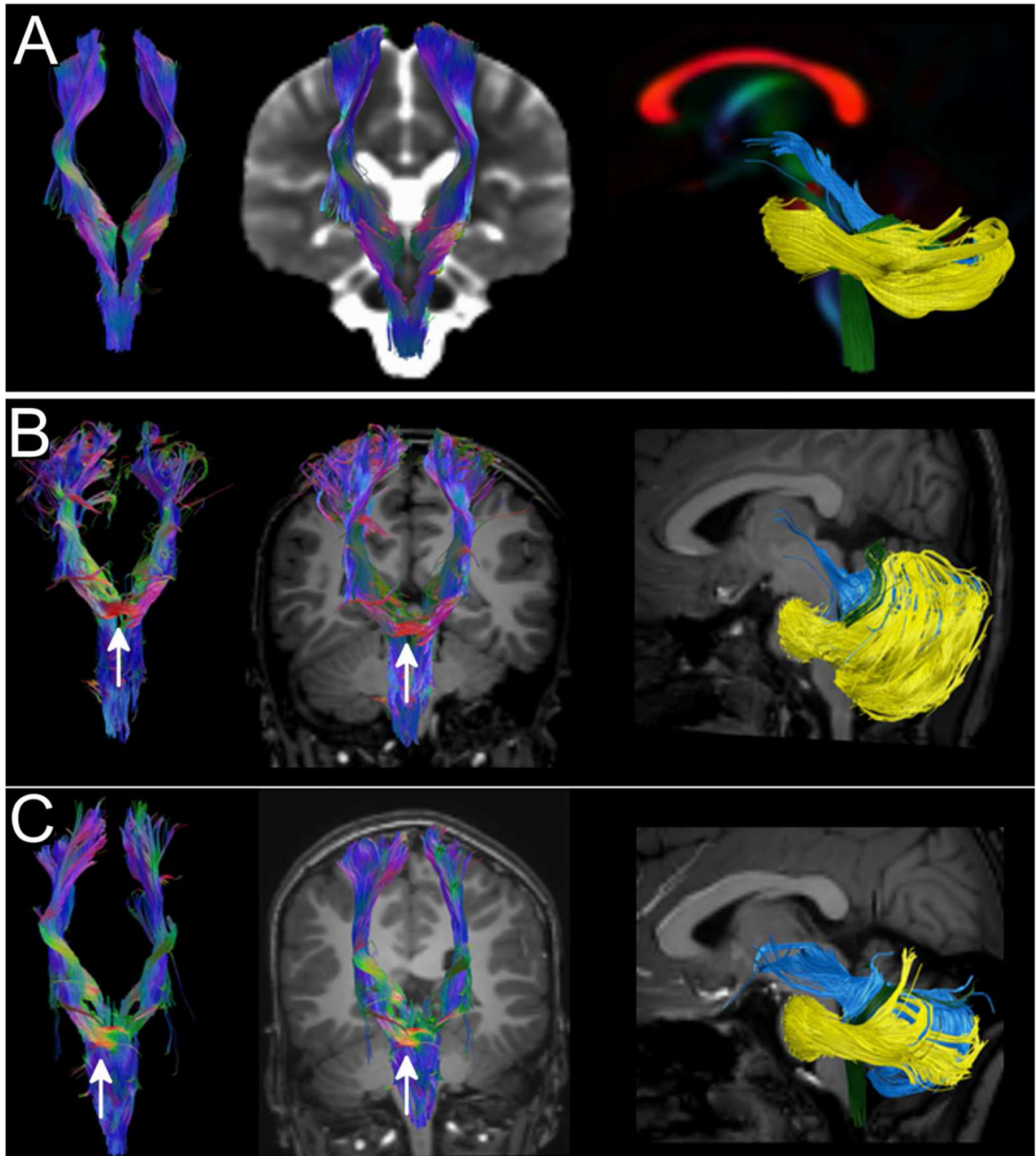


Figure 3. Tractography

CST (first 2 columns) and cerebellar peduncles (last column) were reconstructed using DTI data and FACT algorithm from a template of normal subjects (row A) and in patients 1 and 2 (rows B and C). The ectopic mass seen on morphological sections corresponds to a transvers bundle that seems to be located along CST (white arrow). No transverse fibers are seen in the normal CST at the same level (row A). SCP (light blue tract in the last column) of both patients are thickened, more horizontal than normal and do not pass through the anterior

mesencephalon. Inferior cerebellar peduncles (green tract) in patient 1 are thinned, while, in both patients, middle cerebellar peduncles (yellow tract) are displaced anteriorly in the pons.